Integrated Circuitry to Detect Slippage Inspired by Human Skin and Artificial Retinas

Rocío Maldonado-López, Fernando Vidal-Verdú, Gustavo Liñán, and Ángel Rodríguez-Vázquez, *Fellow, IEEE*

***Abstract*—This paper presents a bioinspired integrated tactile coprocessor that is able to generate a warning in the case of slippage via the data provided by a tactile sensor. Some implementations use different layers of piezoresistive and piezoelectric materials to build upon the raw sensor and obtain the static (pressure) as well as the dynamic (slippage) information. In this paper, a simple raw sensor is used, and a circuitry is implemented, which is able to extract the dynamic information from a single piezoresistive layer. The circuitry was inspired by structures found in human skin and retina, as they are biological systems made up of a dense network of receptors. It is largely based on an artificial retina [22], which is able to detect motion by using relatively simple spatial temporal dynamics. The circuitry was adapted to respond in the bandwidth of microvibrations produced by early slippage, resembling human skin. Experimental measurements from a chip implemented in a 0.35-μm four-metal two-poly standard CMOS process are presented to show both the performance of the building blocks included in each processing node and the operation of the whole system as a detector of early slippage.**

***Index Terms*—Bioinspired chips, slippage detection, tactile sensors.**

I. Introduction

TACTILE sensors are basically arrays of force sensors that emulate biological skin. They are targeted to provide information about texture, stiffness, slippage, friction, and local shape [1]. In many practical applications, these tasks must be completed in *real time* for *large detector arrays*. It is challenging due to the necessity of handling (communication, processing, and storage) many data. These challenges can be undertaken by placing a *parallel-processing* circuitry close to the detectors. The contribution of this circuitry makes the amount of data to decrease and, hence, the overall system efficiency to increase [2]–[8]. Also, the number of long-distance wires between the detectors and the central decision unit is made to decrease, thus easing the embedding of tactile sensors into hands and grippers.

This paper reports building blocks to implement *early tactile* processing tasks and an application-specific integrated circuit (ASIC) for *slippage* detection. Such blocks and the ASIC can be used for different applications.

For instance, *dexterous manipulation* with a robotic hand requires large and conformable sensors. Typical implementations employ flexible raw sensors whose data are read and preprocessed by a circuitry composed of a multiplexor, some analog parts, and an embedded microcontroller [5], [6]. However, this architecture shows limitations to detect slippage. One strategy to overcome these limitations consists of increasing the complexity of the raw sensor—e.g., by adding a layer of a piezoelectric material. Alternatively, ASICs based on the circuits in this paper can replace the multiplexor and the analog parts so that no piezoelectric layer is required to detect slippage. The idea of using ASICs at the interface has been explored elsewhere [3]; however, the chip in [3] does not perform slippage detection.

Other applications such as *minimal invasive surgery* require a small tactile array of sensors and, hence, compact systems. They can be realized by using microelectromechanical system (MEMS) devices. Many tactile sensors based on this technology have been reported [9]–[16]. Most of them implement the array of sensors, together with some circuitry to address and read the data on the same chip [5], [17]. A few authors add a circuitry to preprocess data and perform tasks like edge or texture detection [9], [18]. A recent study [20] reports a hybrid approach based on a MEMS device plus an ASIC that implements a cellular neural network [21] to detect slippage. The ASIC in this paper has been devised for a hybrid architecture where the raw sensors are based on a piezoresistive material. The circuits in this paper could also be implemented on the same substrate of a MEMS device to get a single chip solution.

This paper shows that solutions originally proposed for *silicon retinas* apply to tactile signals as well. Silicon retinas [22]–[25] consist of a 2-D array of locally interconnected identical elementary processing elements (PEs), including not only processing but also sensing capabilities. They operate in parallel manner and are hence well suited for demanding real-time processing tasks that involve operations with relaxed accuracy requirements. Their advantages for handling 2-D data render them suitable candidates for early tactile processing. Also, in vision sensors, as well as in tactile sensors, extracting relevant information requires interactions across the data array. Finally, the ability of silicon retinas to detect temporal changes in an image renders them well suited for slippage detection.

The aim of a slippage detection application is the rapid notification of slippage of an object while being manipulated—e.g.,

Manuscript received July 31, 2008.. First published October 31, 2008; current version published August 12, 2009. This work was supported in part by Spanish Research Projects TEC2006-12376-C02-01 and DIVISA TEC2006-15722. This paper was recommended by Associate Editor A. van Schaik.

F. Vidal-Verdú is with the Department of Electronics, Campus de Teatinos, Universidad de Malaga, 29071 Malaga, Spain (e-mail: fvidal@uma.es).

R. Maldonado-López was with IMSE, 41012 Seville, Spain. She is now with EMPA, Swiss Federal Laboratories for Material Testing and Research, Structural Engineering Research Laboratory, CH-8600 Duebendorf, Switzerland (e-mail: rocio.maldonado-lopez@empa.ch).

G. Liñán, and Á. Rodríguez-Vázquez are with the Department of Analog and Mixed-Signal Circuit Design, Institute of Microelectronics of Seville (IMSE), National Microelectronics Center (CNM), Spanish Microelectronics Center (CSIC), 41012 Seville, Spain (e-mail: angel@cnm.us.es).

Digital Object Identifier 10.1109/TCSI.2008.2008290

by a robot. In the case of a translation, slippage takes place if the following condition is met:

$$f_t/f_n \geq \mu \tag{1}$$

where μ is the friction coefficient and f_t and f_n are the tangential and normal forces at the contact area, respectively. This equation can be employed as a first method detecting the occurrence of slippage. However, it requires precise knowledge of the friction coefficient, which is typically unknown and has to be measured or estimated [26] beforehand. Some implementations train an artificial neural network to detect slippage without an explicit estimation of μ, but the results and their applicability are limited because of the large number of variables involved [27]. A sensor that is capable of measuring f_t and f_n is reported in [20]. In that paper, slippage is detected by identifying the sudden changes in f_t when slippage is produced.

A different approach relies on the detection of the mechanical microvibrations that appear in the early stages of the slippage process. Considering the human analogy, human skin relies on mechanoreceptors to detect slippage [28]. Signals from the fast-adapting (FA) nerve endings indicate the earliest stages of slippage (early slippage) [29], which are followed by an unconscious increase in the grasp force to prevent further slippage. These vibrations are generated by the sequence of stick-slip cycles during slippage, when the surface at the contact area between the indenter and the manipulated object stretches (stick) until the slippage condition in (1) is met and then snaps back (slip). Dynamic sensors or accelerometers can be employed to detect such vibrations [29]. However, this method is extremely sensitive to environmental interferences, such as those generated in the course of multifinger manipulation [27]. Moreover, the robot fingertip cannot house many devices without causing mechanical interference between them [30]. Finally, since these microvibrations are located in the peripheral area of the contact [30], the use of many dynamic devices instead of just one is seemingly more adequate in order to get an earlier and more reliable detection. Furthermore, early slippage is a local phenomenon [31] and hence needs to be detected locally by means of an array of sensors. In addition, it has been observed that the neural response of skin mechanoreceptors encodes the change in local shape from an offset level rather than the absolute force or pressure distribution [32]. This extends the useful operating range and allows the skin to sense features in very irregular objects and in surfaces with different textures.

This paper presents a chip that implements a circuitry whose architecture is inspired on silicon retinas and whose building blocks are adapted to detect microvibrations caused by slippage. This results in a bioinspired chip that resembles the properties of human skin. Some basic ideas, supported by simulations, were previously reported by the authors in [33]. This paper complements [33] by reporting experimental results obtained from the fabricated chip and the associated experimental setup. Also, this paper presents discussions prompted by the measured results and in-depth findings related to the problem. For further details about architectural considerations and electrical design, interested readers can consult [33].

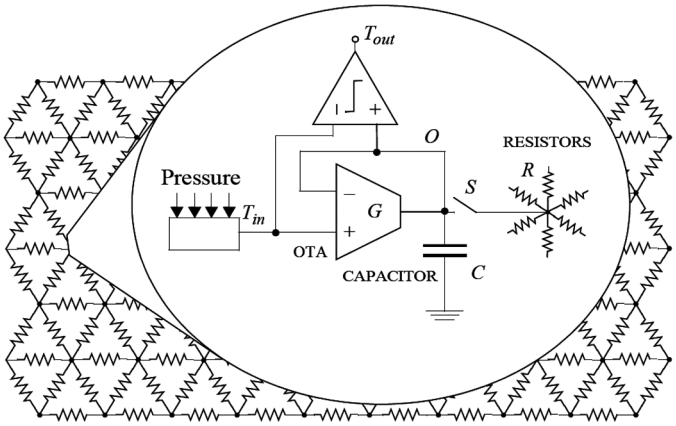

Fig. 1. Proposed architecture is based on silicon retinas in [22] and [23].

II. Architecture

We focused on the architecture of Fig. 1 to design the chip. If the switches (S in Fig. 1) are closed, this architecture corresponds to the well-known silicon retina reported in [22]. The resistive grid and capacitors (C in Fig. 1) produce a spatial temporal local average at node O in Fig. 1. Equations related to it can be found in [22]. The use of local averages allows the retina to detect features in areas of an image under very different lighting conditions and shows a behavior, with respect to local response, similar to that described in Section I for the mechanoreceptors in the skin.

Another interesting alternative to produce local references consists of employing only temporal information, as in purely temporal retinas, such as that reported in [23]. In our architecture, this is obtained if the switches in Fig. 1 are kept open (then the resistive grid is left isolated). In this case, the capacitor stores the past history of the force given by

$$O(s) = \frac{1}{1 + sC/G} T_{\text{in}}(s) \tag{2}$$

which corresponds to the output of the leaky integrator (or low-pass filter) implemented by the operational tranconductance amplifier (OTA) and the capacitor. The output of the cell is obtained by the comparator as

$$T_{\text{out}}(s) = \text{sign}\left[O(s) - T_{\text{in}}(s)\right] \tag{3}$$

thus resulting in a comparison between the current input and its history stored in C, which is easily found to be

$$T_{\text{out}}(s) = \text{sign}\left[\frac{sC/G}{1 + sC/G} T_{\text{in}}(s)\right]. \tag{4}$$

Thus, the output of the cell is simply an indication of the high-pass-filtered version of the input, with the time constant $\tau = C/G$.

From another point of view, one can take this output as an indicator of the time derivative of the input. This simple circuit meets our requirements because it has a local reference and its output is very sensitive to changes in the derivative of the input signal, like those caused by the microvibrations in the stick-slip process observed in early slippage. Notification of this early

slippage takes the form of a train of pulses at the output corresponding to the high number of sign changes in this derivative. It is worth mentioning that the notification of slippage by firing pulses resembles the operation of the biological dynamic mechanoreceptors in the nervous system. Although this is not a consequence of the exact replication of the biological receptor, it has an attractive similarity to this bioinspired approach.

III. Building Blocks

In this section, we present an overview of the main design considerations for the electronic implementation of the different building blocks employed in the design of the tactile PE. Readers are referred to our previous work in [33] for a more detailed description of the electronic design.

From the point of view of implementation, perhaps the most relevant aspect in the design of the blocks in Fig. 1 is the requirement on the time constant $\tau = C/G$. Its value must be chosen such that the high-pass filter dumps the vibrations of frequencies below those observed in the microvibrations. It has been observed [33] that there is a significant response between 60 and 220 Hz. This is also the frequency range where the dynamic mechanoreceptors of biological skin have maximum sensitivity [28]. Thus, in order to filter changes at the input signal due to normal operation, or even due to mechanical vibrations of the robot arms during manipulation, our circuit should have a filter 3-dB frequency of 60 Hz.

The implementation of such a large value of τ implies either an ultralarge capacitance C, an ultrasmall transconductance G (Fig. 1), or both. It is well known that when very long time constants are required, the most frequent and convenient solution relies upon the use of discrete-time switched-capacitor (SC) filters where time constants are not simply defined by the values of the capacitances but also by the capacitor switching frequency [34]. However, this common solution is not best suited for our problem due to several reasons, namely, the area overhead introduced by antialiasing filters, the distribution of the clock(s) to a large array of tactels, and the switching noise introduced in the substrate near the sensing nodes (since the signal from the tactile sensor is very small). Furthermore, the implementation of this SC solution becomes very complex when the tactels need to be dynamically coupled, which is the case in Fig. 1 when the switches are closed. A continuous-time implementation of the PE was opted for due to the large number of input channels in our system and the special requirements (reduced area and power and moderate accuracy of ∼7–8 equivalent bits) in the implementation of topographic processors.

A. Resistive Grid

The coupling resistors in Fig. 1 have been implemented, as shown in Fig. 2(a). This takes up much less area than a network made of passive resistors. Moreover, it is also simpler than the horizontal resistor reported in [22]. After calculations, one can find that this structure presents an equivalent conductance of half the conductance of transistor M_R given by [37]

$$g_{o(M_R)} = n\mu_0 C_{\text{ox}} \frac{W_{M_R}}{L_{M_R}} \sqrt{\frac{2I_r L_{M_C}}{n\mu_0 C_{\text{ox}} W_{M_C}}}. \tag{5}$$

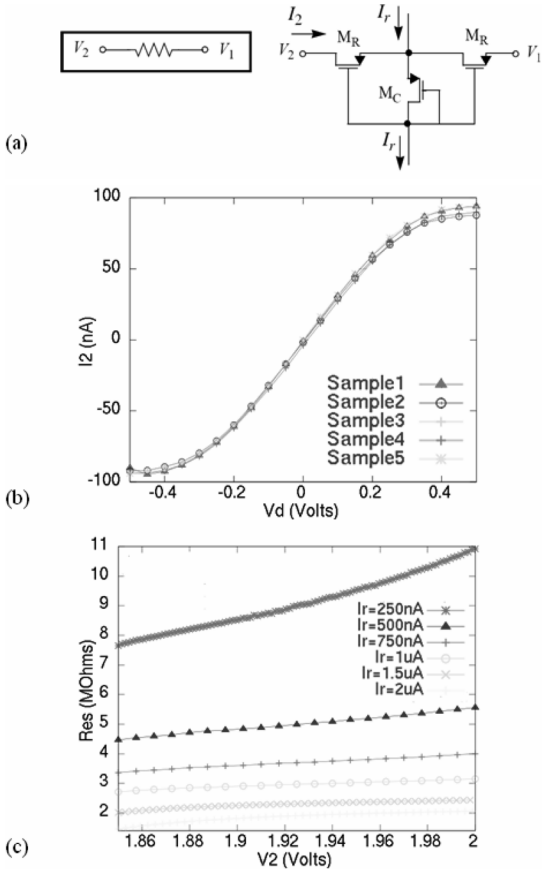

Fig. 2. Active resistor. (a) Schematic. (b) I–V characteristic ($Vd = V2 - V1$). (c) Resistance for different values of the bias current I_r.

Fig. 2(b) shows the obtained I-V characteristic of the resistor for five different chips. Finally, Fig. 2(c) shows the equivalent resistance obtained and how this resistance can be varied by modifying the bias current I_r.

B. Very Low Transconductance OTA

The following three main design options [32] have been taken in order to obtain the required very low transconductance OTA whose schematic is shown in Fig. 3(a): 1) to employ a pMOS differential pair as the core; 2) to incorporate a current division technique in order to reduce the equivalent transconductance further; and 3) to add source degeneration in the OTA main differential pair, which simultaneously reduce the transconductance and expand the linear range. Other strategies to reduce the transconductance employ floating-gate transistors or bulk-driven transistors in the differential pair. However, the OTA in Fig. 3 has a better performance, particularly in terms of area consumption [37].

The transconductance is hence found to be

$$G = \frac{g_{m(M_i)}}{1 + \frac{(M+1)g_{m(M_i)}}{g_{o(M_R)}}} \tag{6}$$

where M_i is the unit transistor in the array of M elements in the differential pair and $g_{o(M_R)}$ is the conductance of transistor M_R given by (5) (with $I_r = I_{rO}$).

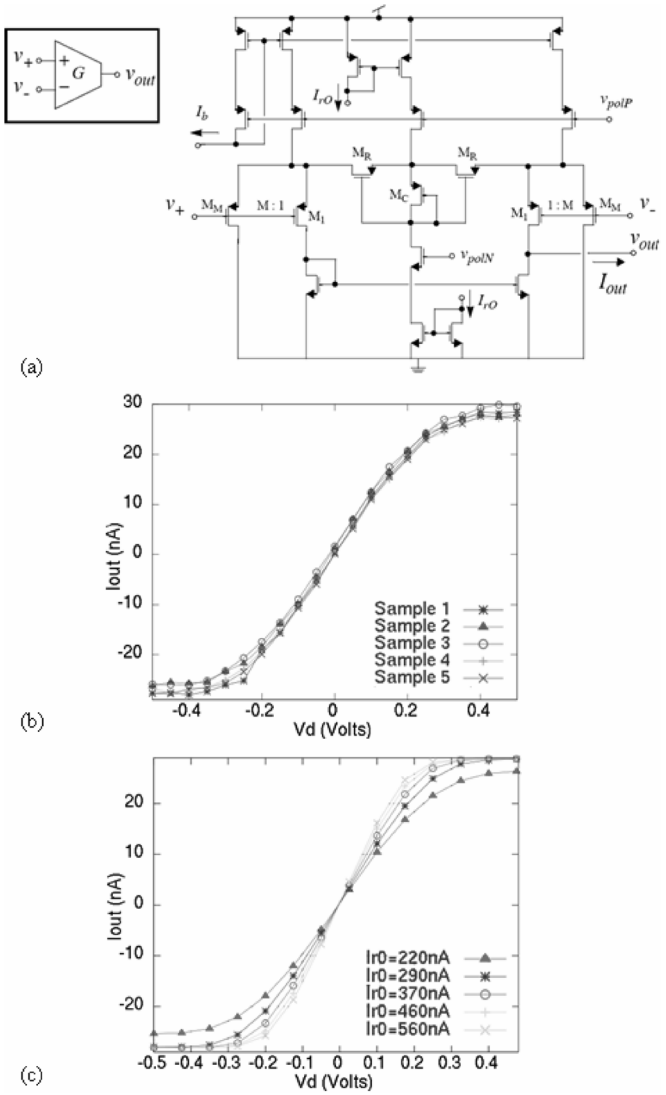

Fig. 3. Very low transconductance OTA. (a) Schematic. (b) I–V characteristic for five samples ($M = 10$ and $Vd = v_+ - v_-$). (c) I–V characteristic for different values of the bias current I_{rO}.

The experimental I–V characteristic curve of the OTA has been measured by employing a semiconductor parameter analyzer. The result is shown in Fig. 3(b), where the curves from five samples are plotted. Finally, Fig. 3(c) shows how the transconductance of the OTA can be controlled by varying its bias current I_{rO}. In our case, a bias current of $I_{rO} = 220$ nA produces a transconductance of 104 nS. The input-referred offset voltage remains below 10 mV in all cases.

C. Implementation of a Large Capacitance

Having a first-order Gm–C filter with a transconductance in the range of 100 nS and a required 3-dB frequency around 60 Hz implies the use of a capacitance of about 270 pF. The direct implementation of such a capacitance using double-poly capacitors (which provide the largest capacitance density per area unit) results in a capacitor of about 3×10^5 μm^2, which is completely unfeasible when one needs to design an array of many tactels, with one such huge capacitor on each of them. Thus, instead of using a purely passive option for the capacitor, we decided to implement an active impedance scaler [36], [37], as shown in Fig. 4(a).

This structure, which also relies on a current division technique, produces an equivalent impedance that is approximately given by

$$Z_i(s) = \frac{v_i}{i_i} \approx \frac{1}{s(N+1)C}. \tag{7}$$

In this paper, we have chosen a capacitance (C) of 27.5 pF and a value of ten for the gain of the impedance scaler (N), which, according to (7), results in an equivalent capacitance of 302.5 pF.

In order to measure this value, we have used a simple RC filter shown in Fig. 4(b). A direct measurement is not possible because the circuit has to be properly biased to work as expected. We measure instead the response of the RC filter with an external passive resistance and the impedance scaler as the capacitor. The input for that circuit is a sinusoidal wave added to an offset. This offset biases the circuit, and the sinusoidal signal enables us to measure the response for different frequencies. We have repeated these measurements for different values of resistor R. The Bode plots that are obtained are shown in Fig. 4(c). Taking into account the cutoff frequency measured for every resistor value, the experimentally measured capacitance is, in all cases, around 300 pF. This result is coherent with the theoretical expected value.

D. Time Constant and Output

This section is devoted to showing the performance of the whole isolated tactel enclosed in an ellipse in Fig. 1 (switch S open), particularly in regard to the main requirement of implementing a large time constant. Fig. 5 shows results for the frequency response of the whole OTA–impedance scaler block, as measured in the laboratory. Specifically, Fig. 5(a) shows the response of the circuit to a linear frequency sweep of 500-Hz spam of the sinusoidal input. Moreover, the gain versus frequency plot for this circuitry for three sinusoidal signals of 100-mV amplitude and 600-mV, 1.4-V, and 2.2-V dc offset, respectively, is shown in Fig. 5(b). Finally, Fig. 5(c) shows this plot for five samples and a similar input with 1.4-V dc offset (note that the input provided by the raw sensor is a microvibration added to a dc offset corresponding to the static pressure).

It is interesting to mention here that we decided to balance the amount of current division in the OTA with that in the capacitor. It is obvious that a lower G could have been obtained by adding more division in the current in the OTA, and hence, we might have employed a smaller capacitor (either a small passive component or a smaller current division) in order to obtain the same time constant. However, having a large division coefficient unavoidably leads to larger mismatching too, and therefore, since precision is to be maintained, it results in a need for bigger transistors. Therefore, we decided to use the same division coefficient in both OTA and impedance scaler structures and, consequently, to design both to exhibit the same relative accuracy. On the other hand, the use of ultralow currents in one of the structures (either G or C) due to an excessively high division factor also makes the system much more sensitive to noise.

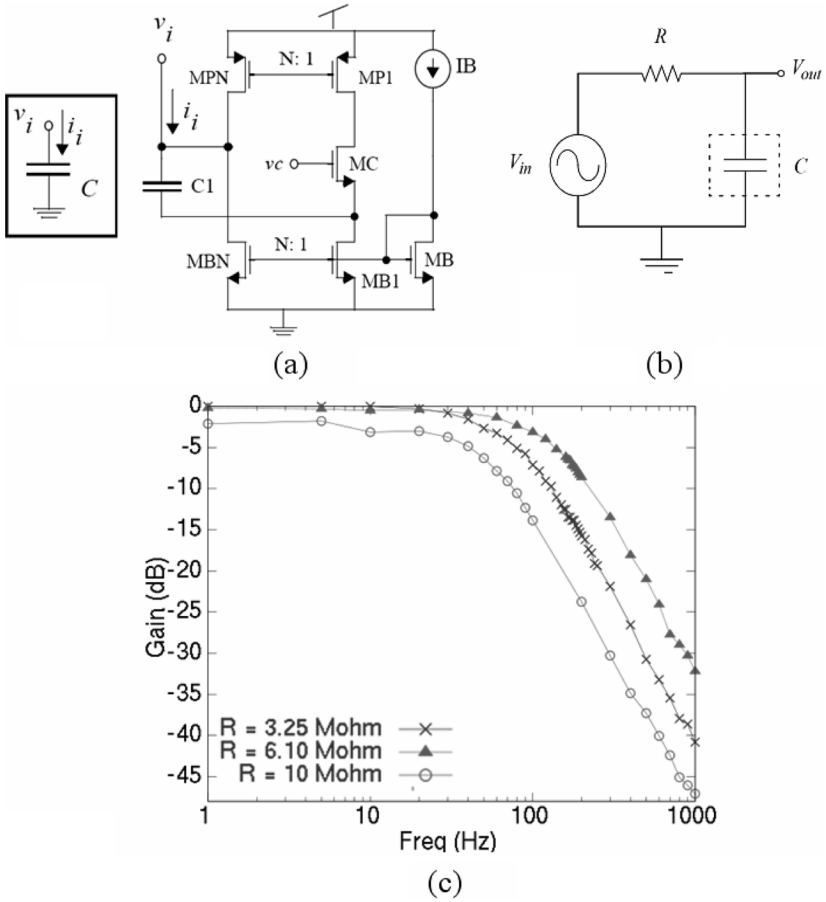

Fig. 4. Impedance scaler. (a) Schematic. (b) RC filter used to estimate C. (c) Bode plot of the RC filter.

The last building block is a comparator placed at the output stage of our tactile sensor as the output amplifier. Thus, we obtain a digital signal because the microvibrations of the sensor output signal, in the range of the frequencies related to slippage, will cause the output signal to oscillate from high to low state, thus generating the train of pulses mentioned in Section II. We have chosen a conventional one-step voltage comparator with a symmetric operational transconductance amplifier comparator structure [38]. We have added some hysteresis to the comparator in order to increase its robustness against noise. Fig. 6 shows the response of the tactel to a linear frequency sweep of the sinusoidal input.

IV. Implementation of the Chip

This section provides a general description of the so-called TPC16 chip, which has been implemented with the architecture and building blocks described in the previous sections. Fig. 7 shows the block diagram and layout of the TPC16 chip. It consists of a 4×4 rectangular array of processing units, which contains the building blocks described in Section III. In addition to this main array and its biasing circuitry, we have implemented a set of isolated building blocks (an impedance scaler, an OTA, and a resistor) for testing purposes. Switches added to the network resistors allow us to choose between different configurations for the matrix of processing units: 16 isolated tactels, 16 tactels in a linear array, or a 4×4 rectangular arranged array. The chip size, including pads, is $2.2 \times 2.2\ \mathrm{mm}^2$, and it has been implemented in a 0.35-μm four-metal two-poly standard CMOS process available through the Europractice IC Service [39].

The layout of a tactel in the TPC16 is shown in Fig. 8. The building blocks in Fig. 1 can be identified. The size of each processing unit is $275 \times 350\ \mu\mathrm{m}$. The impedance scaler is the largest building block representing a percentage of 53% of the total area of the tactel. Specifically, the poly–poly capacitance in the impedance scaler consumes 34% of the area. The OTA, comparator, and each resistor represent 13%, 4.5%, and 1.5% of the area, respectively. Special attention has been paid to the power consumption of the elements in the tactel. The maximum static current consumption is 5 μA.

Looking for flexibility, we have opted for downloading the complete set of outputs from the tactels. However, note that if we are interested in generating a slippage condition warning signal, a simpler approach consists of implementing the comparator with an open collector or open drain output and connecting it to a single line bus ended with a pull-up device. This is logically equivalent to the NOR function of the output signals provided by all the tactels.

V. Experimental Results

Fig. 9 shows the experimental setup used to test the chip. It consists of an inclined plane, with a raw tactile sensor being fixed to its surface. Thus, when an object slides down the inclined plane, our sensor will collect the pressure data derived

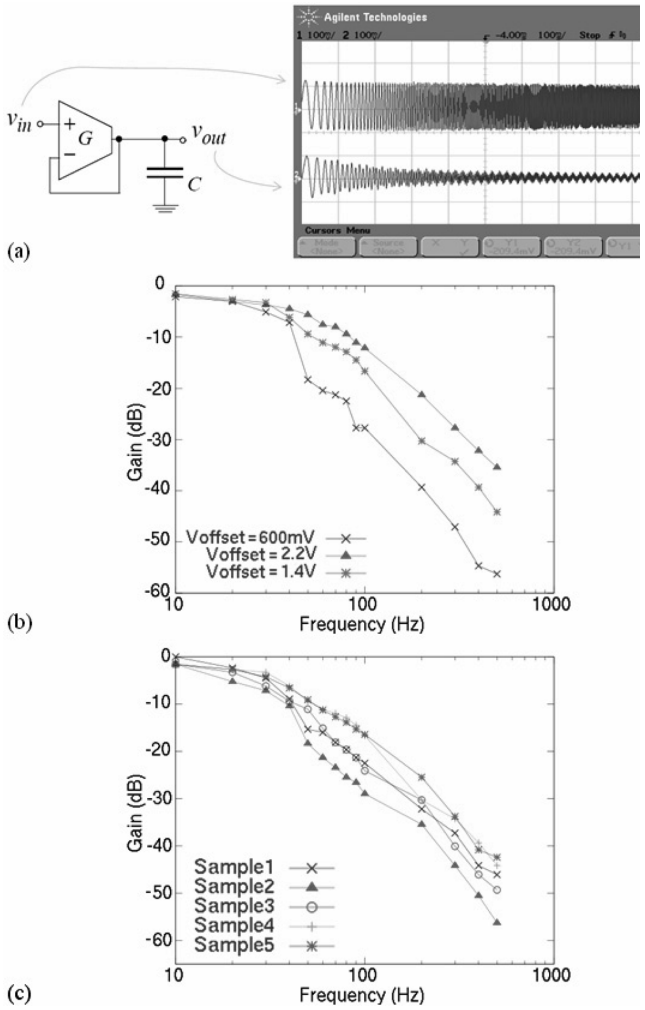

Fig. 5. Measurements to estimate the dynamic response of the $Gm-C$ filter as the main requirement of the tactel. (a) Linear frequency sweep at input. (b) Bode plot for different dc offsets. (c) Bode plot for different samples.

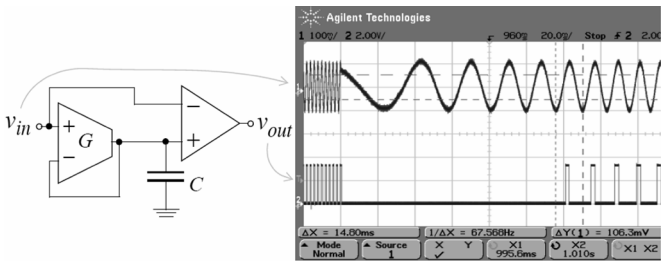

Fig. 6. Response of an isolated tactel to a linear frequency sweep of a sinusoidal input.

from this phenomenon. The raw tactile sensor is a piezoresistive film (from INTERLINK) that has been placed atop a PCB board with a set of comb-shaped electrodes. The result is a linear array with 16 tactels with a separation of 2.54 mm $(0.1'')$. The transduction method is based on the variation of the material resistance when it is pressed, i.e., piezoresistivity.

Since the approach proposed to detect slippage is based on microvibrations at the sensor interface, we have noted that the design of the raw sensor to generate such vibrations is important. Specifically, we have experimentally observed that the approach does not work if the friction coefficient at the interface is too low. The same is true with biological skin, e.g., we do not detect slippage if the skin is covered with oil or sweat. In fact, ridges in the skin that increase this coefficient have been emulated by some sensors in the form of rubber textures or brushing elements [40], [41]. In this paper, we have covered our sensor with a flat elastomer, and another thin elastomer also covers the object that is placed on the sensor in our experiments.

The nodes of the raw sensor present a pressure-dependent resistance as the output parameter. Thus, before being processed by the TPC16, it needs to be converted into a voltage signal. Moreover, a signal conditioning circuit has been implemented, which consists of a set of 16 blocks, each containing two operational amplifiers to condition and amplify the signals obtained from the sensor, with adjustments for control of offset and gain. This conditioning circuit has been placed on a separate PCB board to gain flexibility in the testing process, but it could readily be implemented on a chip in a more advanced prototype.

In addition to the signal conditioning board, a TPC16 test one (bottom of Fig. 9) has been implemented. The main part of this board is the TPC16. The chip receives as input the output signals of the signal conditioning board. The output signals from the TPC16 are stored in a circuit of 4-Mbit SRAM memory capacity and may be sent to the computer via an RS-232 port. The board is governed by an XC2S200E FPGA from Xilinx Inc. Spartan-IIE, which is responsible for controlling the overall system.

The outputs of the chip are digital signals (outputs of comparators), so they can be processed directly by the FPGA without the need of analog-to-digital converters. Specifically, the FPGA is responsible for acquiring signals from the chip to store them in the SRAM memory and then send them to the PC. Also, the FPGA implements an algorithm to generate a unique alarm signal from the trains of pulses from the chip. Since, in practice, a number of spikes are still generated by rolling or noise (either electrical or mechanical), slippage identification is made by counting the edges within a given time interval and comparing this count with a given threshold that could also be adjusted dynamically by a learning process. A similar approach is implemented in [35], where they define three parameters to distinguish slippage from the stable state: 1) minimum number M_P of pulses; 2) maximum time Δ_M between pulses; and 3) minimum number M_T of tactels that accomplish the previous conditions. Thus, if a minimum number M_P of pulses is in a minimum number M_T of tactels, with a separated maximum time Δ_M from one to the other, slippage is noted. We have also implemented this simple algorithm, and slippage triggers the alarm signal and turns on one of the LEDs in the test board. The FPGA also stores the data from the chip and sends them to the computer via a serial port.

Figs. 10 –13 show the experimental results from this setup. They depict the output of a single tactel (a), as well as the OR function on the outputs of the tactels (b). Fig. 10 shows the output when the nodes in the array are coupled with the resistors, so the switches in Fig. 1 are closed (since the movement in our experiment is a linear translation, we have used a linear raw sensor with 16 elements, and we have set the nodes in the

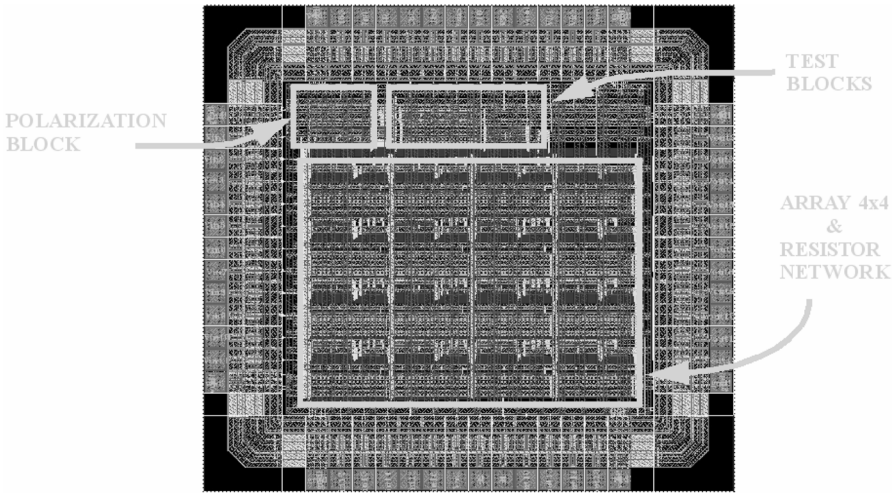

Fig. 7. Block diagram and layout of the TPC16 chip.

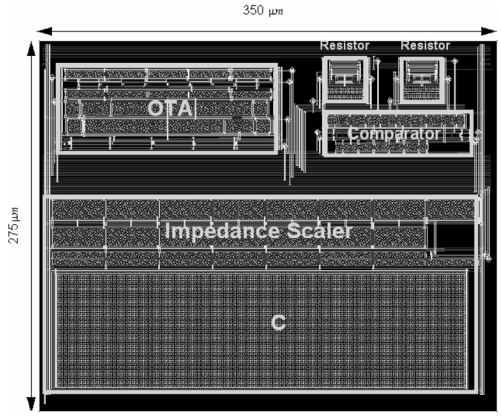

Fig. 8. Layout of a single tactel.

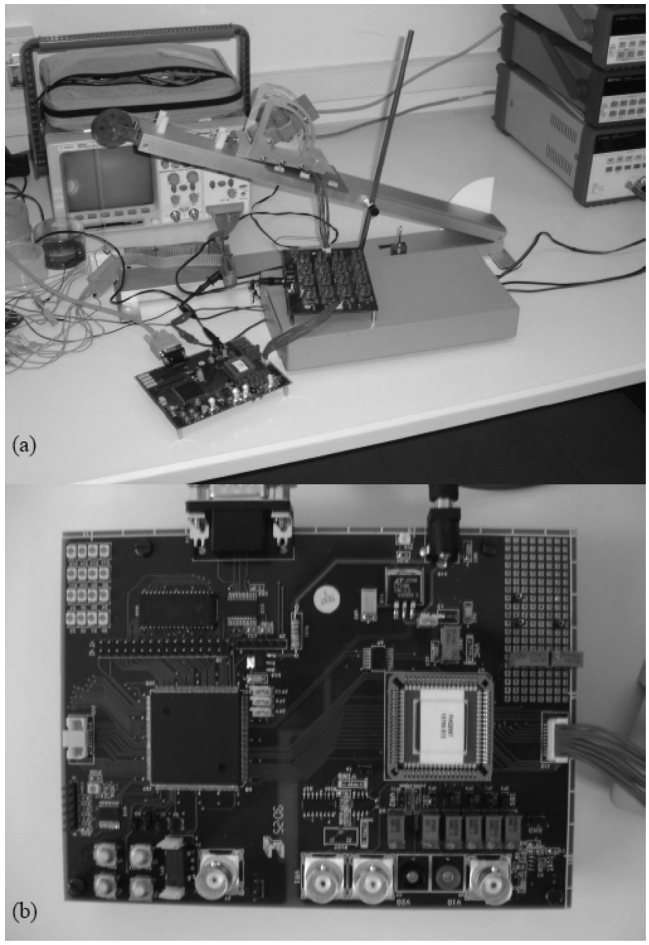

Fig. 9. (a) Experimental setup and (b) test board containing the TPC16 chip.

chip to be a linear array). Fig. 11 shows a similar trial, with the nodes in the chip being isolated, so the switches in Fig. 1 are open. Finally, Figs. 12 and 13 show two trials where a cylinder rolls down the inclined plane with coupled or isolated nodes, respectively. We also observe that no train of pulses is generated when there is no any object on the tactile sensors or when an object is still on the sensor.

Note that a much lower number of edges is registered in the rolling experiments of Figs. 12 and 13 than that in the slippage response in Figs. 10 and 11, and we can distinguish between rolling and slippage at a glance. In the results from the rolling experiments, there are still some edges caused by the sudden pressure step on every tactel of the sensor reached by the cylinder on its downward roll.

Another significant issue is the higher number of edges registered in Fig. 11, when the nodes are isolated, than in Fig. 10, when the nodes are coupled. As mentioned earlier, the resistive network computes a spatial temporal average of the signals provided by the nodes, and hence, the system turns into a spatial temporal filter. In this case, the reference employed by the comparator to decide whether slippage is occurring or not is a local value, depending not only on the past history of the tactel input but also on that of its neighbors. The strength of this dependence is given by the product of the coupling resistance R and the OTA transconductance G (see Fig. 1). The larger the value of G or R, or the distance between two tactels, the lower the influence on each other. If $R \rightarrow \infty$, we get the same case that is obtained for the open switches. For the coupled nodes, the spatial reference O can be far from the input T_{in} for surfaces with irregular shapes, e.g., triangular indenters, so changes in T_{in} cannot be

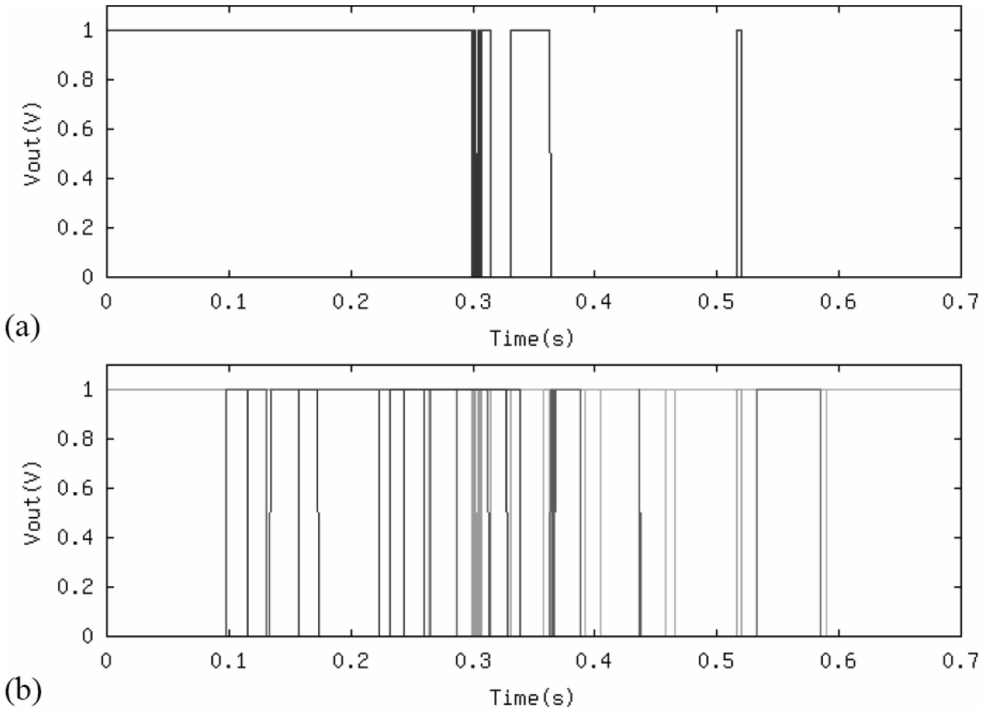

Fig. 10. Response to slip (a) from a single tactel and (b) from the whole set with tactels connected in a linear array.

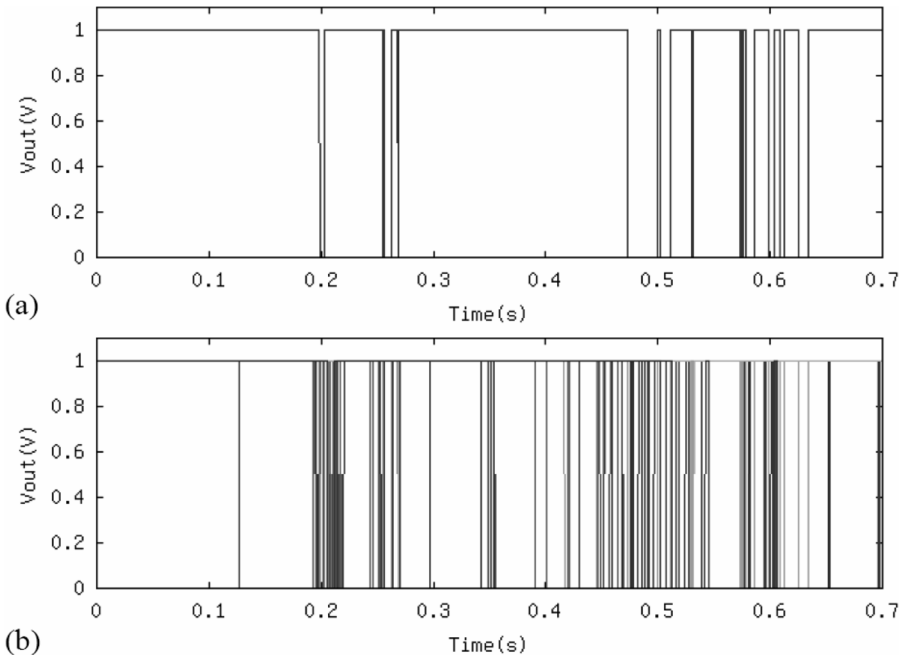

Fig. 11. Response to slip (a) from a single tactel and (b) from the whole set with isolated tactels.

noticeable at the output in (3) because the sign of $O(s) - T_{\text{in}}(s)$ does not change. When the switches are open or $R \rightarrow \infty$ in Fig. 1, $O(s) = T_{\text{in}}(s)$ under static conditions, and any change in the input causes a change in (3) as long as it is not filtered by the dynamic response of the circuit.

In order to highlight this, we carried out a simple experiment. A 200-Hz-frequency, 100-mV-amplitude, and 2-V-dc-offset signal was set at all inputs of the tactels in the chip, except number 12, which was set to 1.5 V. Outputs 8–15 are shown in Fig. 14(a) and (c). The nodes are isolated in Fig. 14(a), while they are linearly coupled in Fig. 14(c). It can be observed that three outputs do not oscillate in the second case, so coupling weakens the response. However, coupling can also strengthen the response. For instance, two plots are shown in Fig. 14(b) and (d) corresponding to the following situations. In Fig. 14(b), we have the nodes isolated when all the inputs are signals of 200-Hz frequency, 100-mV amplitude, and 2-V dc offset, except number 12, which is set to 2-V dc. In Fig. 14(d), we show the response when the nodes are set as a bidimensional 4×4 coupled array. It is observed that all outputs oscillate,

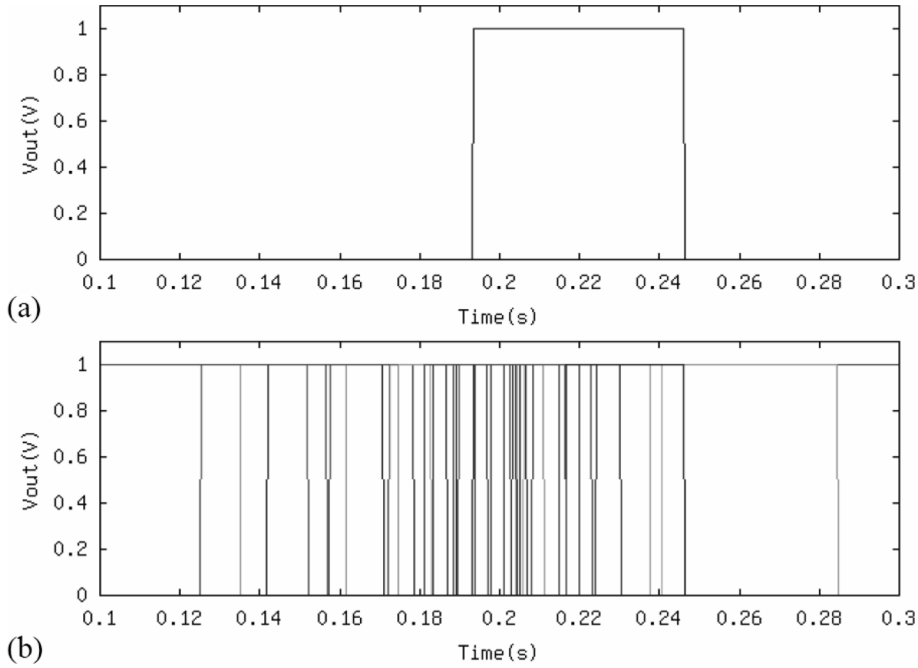

Fig. 12. Response to rolling (a) from a single tactel and (b) from the whole set with tactels connected in a linear array.

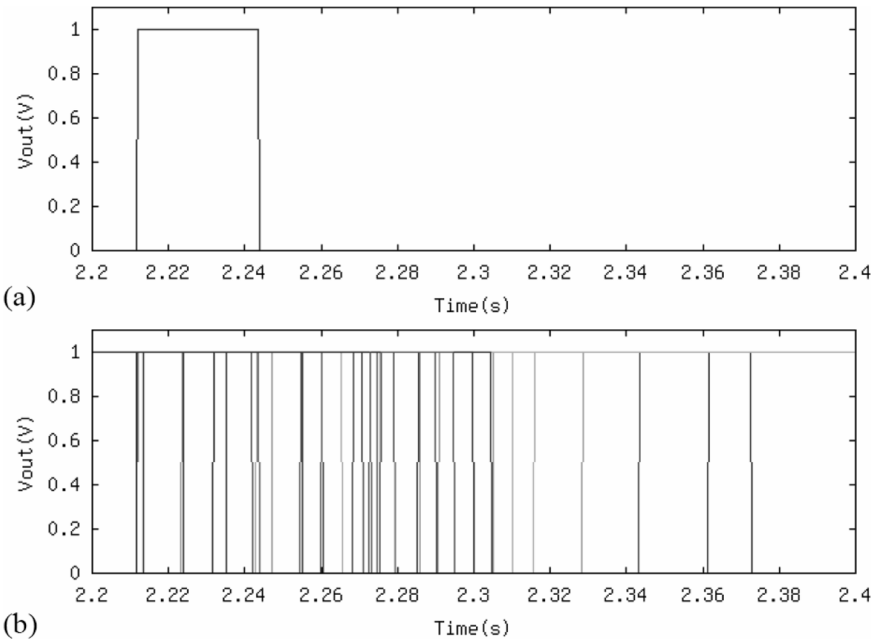

Fig. 13. Response to rolling (a) from a single tactel and (b) from the whole set with isolated tactels.

even number 12, whose associated input does not change. This could be seen as a positive point to strengthen the response to slippage. However, it can also increase the response to false slippage or rolling. This can be the case of Fig. 12, where a higher number of edges is registered than expected. On the contrary, Fig. 13 shows a fewer number of edges, so we could conclude that a larger difference between rolling and slippage is observed when the tactels are isolated.

Let us finally show the performance of the system to detect slippage when the nodes are isolated and the pressure profiles registered by the tactile sensor are uneven, which is the main aim of this paper. We have set the parameters of the slippage detection algorithm in the FPGA in order to detect slippage and discriminate between these two phenomena. The minimum number M_P of pulses has been set to three, with a maximum time Δ_M of separation of 200 ms, and the minimum number M_T of tactels have been set to one. With these parameters, the slippage signal was generated successfully, even when the pressure distribution on the tactile sensor was quite uneven. We built a small trolley that could be configured to generate different pressure profiles. For instance, Fig. 15 shows three different situations. Pressure distribution has been measured with an I-Scan system from Tekscan with a very thin film sensor located under the trolley while it is on the inclined plane. The graphs on the left of

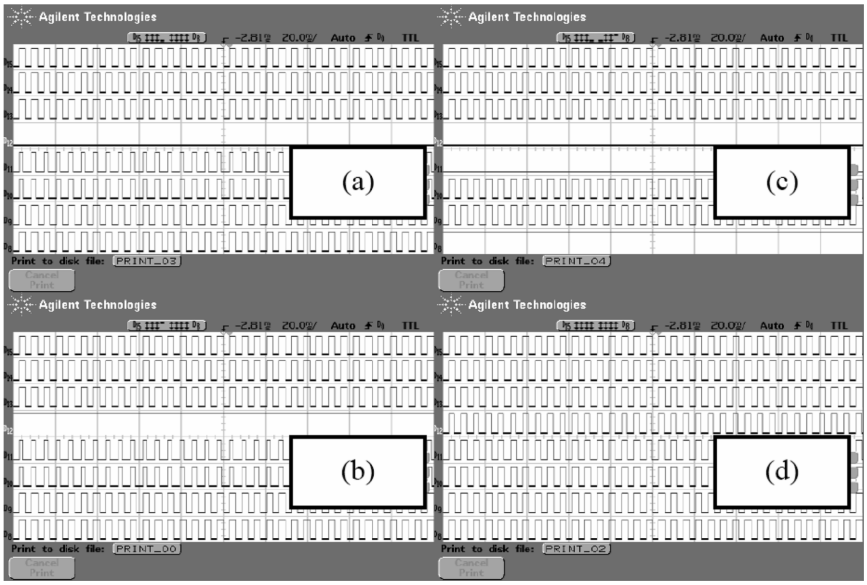

Fig. 14. Outputs of the chip when the inputs are (left) isolated or (right) coupled and the inputs are set to different values (see the text for the explanation).

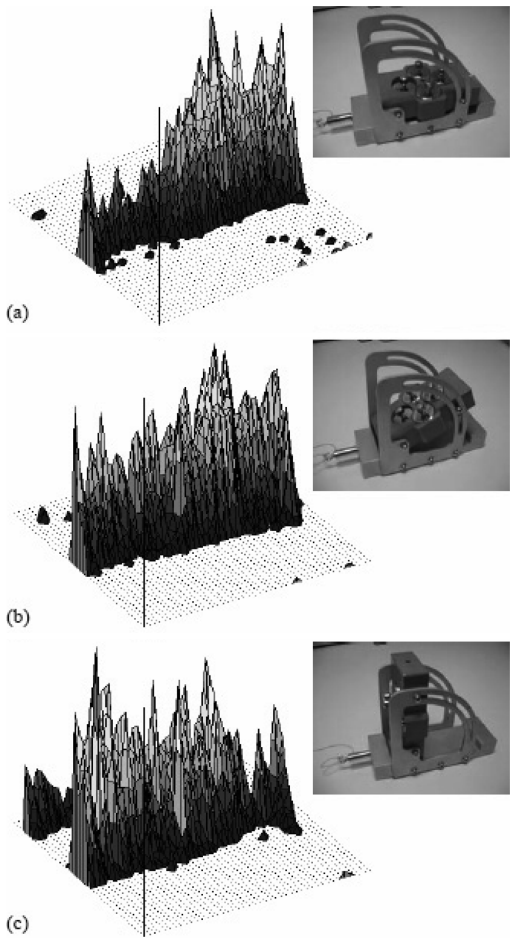

Fig. 15. Different profiles generated by the trolley as measured by the I-Scan system from Tekscan while it is still on the inclined plane.

Fig. 15 show these distributions, while the photographs on the right of Fig. 15 show the trolley, as it is set to get such profiles. It can be observed that, even in Fig. 15(b), where the trolley is configured to get a more uniform pressure profile, it is quite uneven. In all cases, slippage was detected with the nodes in the chip isolated in simple experiments that consisted in releasing the trolley for it to slip down the inclined plane.

We have repeated the experiments, and we have observed that the slippage alarm was triggered in every slippage situation. However, during the rolling experiments, the slippage alarm was not set on. Nevertheless, different situations due to the type of experiment performed or the tactile material employed in each case can lead to different outputs. Thus, it is important to set the parameters of the slippage detection algorithm in the FPGA properly in order to detect slippage and avoid false alarms.

VI. Conclusion

A bioinspired ASIC to detect slip microvibrations was reported. It employed the silicon retina architecture proposed in the seminal work by Prof. C. Mead [22]. We have shown that ideas devised for vision sensors apply to tactile sensors, provided that pertinent parameters are tuned to meet the needs of the slip detection problem. Particularly, the implementation of large time constants is a key issue in the proposed circuit. Measurements from silicon prototypes demonstrate that the building block requirements are met and that the chip is capable of detecting slippage.

The chip can be configured with switches to implement the resistor network presented in [22]; alternatively, it can be configured as an array of isolated nodes resembling a pure temporal artificial retina [23]. Both configurations share the use of a local reference. In the first case, this reference is a spatial temporal average that takes into account the activity of the neighbors of each tactel. In the second case, the reference is the output of the tactel in recent history. In the case of silicon retinas, this local reference was employed to detect local features in images with very different areas in terms of illumination conditions. In the case of tactile sensors, the local reference is employed to report

slip with indenters (for instance, in a grasping task) with different shapes and textures.

We have observed significant differences between the response of the system to slip on the one hand and to rolling on the other hand. These differences appeared in both architectural configurations but were more noticeable if the tactels were isolated. We have also observed that this architecture responded better when the inputs differed largely from each other. Based on our experiments, we did not see any advantage of using the resistor network to detecting slippage. Although this configuration could be beneficial for other preprocessing tasks such as edge detection, for detection of slippage, it is better to implement the simpler case where the tactels are isolated.

The implementation of an additional simple algorithm can help to avoid false warning signals caused by electrical or mechanical noise, and this has also been implemented by other authors [35]. Finally, the experiments show that the approach is valid and can be used to discriminate between slippage and rolling conditions, even in the case of uneven pressure profiles at the contact interface, which is very interesting regarding the manipulation of objects with dexterous robotic hands.

REFERENCES

[1] M. H. Lee and H. R. Nicholls, "Tactile sensing for mechatronics—A state of the art survey," *Mechatronics*, vol. 9, no. 1, pp. 1–31, Feb. 1999.

[2] M. H. Lee, "Tactile sensing: New directions, new challenges," *Int. J. Robot. Res.*, vol. 19, no. 7, pp. 636–643, Jul. 2000.

[3] A. Iwashita and M. Shimojo, "Development of a mixed signal LSI for tactile data processing," in *Proc. IEEE Int. Conf. Syst., Man, Cybern.*, 2004, vol. 5, pp. 4408–4413.

[4] J. Tegin and J. Wikander, "Tactile sensing in intelligent robotic manipulation—A review," *Ind. Robot*, vol. 32, no. 1, pp. 64–70, Jan. 2005.

[5] B. Choi, H. R. Choi, and S. Kang, "Development of tactile sensors for detecting contact force and slip," in *Proc. IEEE Int. Conf. IROS*, Aug. 2005, pp. 2638–2643.

[6] K. Weiss and H. Woern, "Tactile sensor system for an anthropomorphic robotic hand," in *Proc. IEEE Int. Conf. Manipulation Grasping*, Genua, Italy, Jul. 2004, pp. 587–592.

[7] G. Cannata and M. Maggiali, "An embedded tactile and force sensor for robotic manipulation and grasping," in *Proc. 5th IEEE-RAS Int. Conf. Humanoid Robots*, Dec. 2005, pp. 80–85.

[8] D. Göger, K. Weiss, C. Burghart, and H. Wörn, "Sensitive skin for a humanoid robot," in *Proc. 2nd Int. Workshop HCRS*, Munich, Germany, Oct. 2006.

[9] U. Paschen, M. Leineweber, J. Arnelung, M. Schmidt, and G. Zimmer, "A novel tactile sensor for heavy-load applications based on an integrated capacitive pressure sensor," *Sens. Actuators A, Phys.*, vol. 68, no. 1–3, pp. 294–298, Jun. 1998.

[10] M. Leineweber, G. Pelz, M. Schmidt, H. Kappert, and G. Zimmer, "New tactile sensor chip with silicone rubber cover," *Sens. Actuators A, Phys.*, vol. 84, no. 3, pp. 236–245, Sep. 2000.

[11] R. S. Dahiya, M. Valle, G. Metta, and L. Lorenzelli, "POSFET based tactile sensor arrays," in *Proc. 14th IEEE Int. Conf. Electron., Circuits Syst.*, Marrakech, Morocco, Dec. 2007, pp. 1075–1078.

[12] H.-K. Lee, S.-I. Chang, and E. Yoon, "A capacitive proximity sensor in dual implementation with tactile imaging capability on a single flexible platform for robot assistant applications," in *Proc. 19th Int. Conf. MEMS*, Istanbul, Turkey, Jan. 2006, pp. 606–609.

[13] D. V. Dao, Q. Wang, and S. Sugiyama, "Fabrication and characterization of 3-DOF soft-contact tactile sensor utilizing 3-DOF micro force moment sensor," *IEEJ Trans. Sens. Micromachines*, vol. 127, no. 3, pp. 177–181, 2007.

[14] G.-S. Chung, "Fabrication and characteristics of Si piezoresistive micropressure sensors for tactile imaging devices," *J. Korean Phys. Soc.*, vol. 49, no. 1, pp. 37–41, Jul. 2006.

[15] H. Takao, K. Sawada, and M. Ishida, "Multifunctional smart tactile-image sensor with integrated arrays of strain and temperature sensors on single air-pressurized silicon diaphragm," in *Proc. 13th Int. Conf. Solid-State Sens., Actuators, Microsyst.*, Seoul, Korea, Jun. 2005, pp. 45–48.

[16] J. Engel, N. Chen, C. Tucker, C. Liu, S.-H. Kim, and D. Jones, "Flexible multimodal tactile sensing system for object identification," in *Proc. IEEE Sens.*, Daegu, Korea, Oct. 2006, pp. 563–566.

[17] D. Johnston, P. Zhang, J. Hollerbach, and S. Jacobsen, "A full tactile sensing suite for dexterous robot hands and use in contact force control," in *Proc. IEEE Int. Conf. Robot. Autom.*, Apr. 1996, vol. 4, pp. 3222–3227.

[18] M. H. Raibert and J. E. Tanner, "Design and implementation of a VLSI tactile sensing computer," *Int. J. Robot. Res.*, vol. 1, no. 3, pp. 3–18, 1982.

[19] M. Shimojo and M. Ishikawa, "An active touch sensing method using a spatial filtering tactile sensor," in *Proc. IEEE Int. Conf. Robot. Autom.*, 1993, pp. 948–954.

[20] A. Kis, F. Kovács, and P. Szolgay, "3-D tactile sensor array processed by CNN-UM: A Fast method for detecting and identifying slippage and twisting motion," *Int. J. Circuit Theory Appl.*, vol. 34, no. 4, pp. 517–531, Jul. 2006.

[21] L. O. Chua, *CNN: A Paradigm for Complexity*. Singapore: World Scientific, 1998.

[22] C. Mead, *Analog VLSI and Neural Systems*. Reading, MA: Addison-Wesley, 1989.

[23] P. Lichtsteiner, C. Posch, and T. Delbruck, "A 128 × 128 120 dB 15 ms latency asynchronous temporal contrast vision sensor," *IEEE J. Solid-State Circuits*, vol. 43, no. 2, pp. 566–576, Feb. 2008.

[24] R. Carmona-Galan, F. Jimenez-Garrido, C. M. Dominguez-Mata, R. Dominguez-Castro, S. E. Meana, I. Petras, and A. Rodriguez-Vazquez, "Second-order neural core for bioinspired focal-plane dynamic image processing in CMOS," *IEEE Trans. Circuits Syst. I, Reg. Papers*, vol. 51, no. 5, pp. 913–925, May 2004.

[25] A. Rodriguez-Vazquez, G. Linan-Cembrano, L. Carranza, E. Roca-Moreno, R. Carmona-Galan, F. Jimenez-Garrido, R. Dominguez-Castro, and S. E. Meana, "ACE16k: The third generation of mixed-signal SIMD-CNN ACE chips toward VSoCs," *IEEE Trans. Circuits Syst. I, Reg. Papers*, vol. 51, no. 5, pp. 851–863, May 2004.

[26] C. Melchiorri, "Slip detection and control using tactile and force sensors," *IEEE/ASME Trans. Mechatronics*, vol. 5, no. 3, pp. 235–243, Sep. 2000.

[27] G. Canepa, R. Petrigliano, M. Campanella, and D. De Rossi, "Detection of incipient object slippage by skin-like sensing and neural network processing," *IEEE Trans. Syst., Man, Cybern. B, Cybern.*, vol. 28, no. 3, pp. 348–356, Jun. 1998.

[28] R. D. Howe and M. R. Cutkosky, "Sensing skin acceleration for slip and texture perception," in *Proc. IEEE Robot. Autom.*, 1989, pp. 145–150.

[29] R. D. Howe, "Tactile sensing and control of robotic manipulation," *J. Adv. Robot.*, vol. 8, no. 3, pp. 245–261, 1994.

[30] I. Fujimoto, Y. Yamada, T. Morizono, Y. Umetani, and T. Maeno, "Development of artificial finger skin to detect incipient slip for realization of static friction sensation," in *Proc. IEEE Multisensor Fusion Integr. Intell. Syst.*, 2003, pp. 15–21.

[31] S. A. Stansfield, "Experiments in robotic sensorimotor control during grasp," *IEEE Trans. Syst., Man, Cybern.*, vol. 23, no. 3, pp. 891–896, May/Jun. 1993.

[32] W. J. Peine and R. D. Howe, "Do humans sense finger deformation or distributed pressure to detect lumps in soft tissue?," *Proc. ASME Dyn. Syst. Control Division*, vol. 64, pp. 273–278, 1998.

[33] R. Maldonado-López, F. Vidal-Verdú, G. Liñán, E. Roca, and Á. Rodríguez-Vázquez, "Early slip detection with a tactile sensor based on retina," *Analog Integr. Circuits Signal Process.*, vol. 53, no. 2/3, pp. 97–108, Dec. 2007.

[34] P. E. Allen and E. Sánchez-Sinencio, *Switched Capacitor Circuits*. New York: Van Nostrand Reinhold, 1984.

[35] T. Matsumiya, S. Nakayama, Y. Miura, P. Chen, and T. Toyota, "Intelligent control method for robot hand based on tactile information," in *Proc. IEEE Int. Conf. Syst., Man, Cybern.*, 1999, pp. 768–773.

[36] J. Silva-Martínez and S. Solís-Bustos, "Design considerations for high performance very low frequency filters," in *Proc. IEEE ISCAS*, 1999, vol. 2, pp. 648–651.

[37] A. Veeravalli, E. Sánchez-Sinencio, and J. Silva-Martínez, "Transconductance amplifier structures with very small transconductances: A comparative design approach," *IEEE J. Solid-State Circuits*, vol. 37, no. 6, pp. 770–775, Jun. 2002.

[38] A. Rodríguez-Vázquez, M. Delgado-Restituto, and R. Domínguez-Castro, "Comparators: Architectures for voltage and current input with CMOS implementation examples," in *Wiley Encyclopedia of Electrical and Electronics Engineering*. New York: Wiley, 1999, vol. 3, pp. 557–600.

[39] [Online]. Available: http://www.europractice-ic.com

[40] P. A. Schmidt, E. Maël, and R. Würtz, "A sensor for dynamic tactile information with applications in human–robot interaction and object exploration," *Robot. Auton. Syst.*, vol. 54, no. 12, pp. 1005–1014, Dec. 2006.

[41] J. Jockusch, J. Walter, and H. Ritter, "A tactile sensor system for a three-fingered robot manipulator," in *Proc. ICRA*, 1997, pp. 3080–3086.

Rocío Maldonado-López received the Telecommunication Engineer degree from the University of Seville, Seville, Spain, in 2004. Since 2004, she has been working toward the Ph.D. degree with the Department of Analog and Mixed-Signal Circuit Design, Microelectronics Institute of Seville (IMSE), National Microelectronics Center (CNM), Spanish Microelectronics Center (CSIC). In 2006, she received the Diploma of Advanced Studies in Microelectronics from the University of Seville for the research project entitled "Design of Bioinspired Tactile Processing Chips."

In 2005, she received a scholarship from the Spanish Council of Scientific Research (CSIC) to continue researching at IMSE. She is currently working at EMPA, Swiss Federal Laboratories for Material Testing and Research, with the Laboratory of Structural Engineering Research, Duebendorf, Switzerland. Her main areas of interest include the design and test of analog- and mixed-signal chips, advanced tactile sensors, and tactile signal processing and applications.

Fernando Vidal-Verdú received the B.S. degree in physics–electronics from the University of Seville, Seville, Spain, in 1988 and the Ph.D. degree in microelectronics from the University of Málaga, Málaga, Spain, in 1996.

From September 1988 to April 1991, he was with the Department of Electronics and Electromagnetism, School of Engineering, University of Seville, for a project supported by Fujitsu España S.A. In May 1991, he joined the University of Málaga as a Profesor Ayudante, where he is currently a Profesor Titular (Associate Professor) with the Department of Electronics. He is the author or coauthor of 20 papers in international journals and chapters of books and more than 40 papers in conference proceedings. His research interests include circuits and systems for tactile interfaces.

Gustavo Liñán received the Licenciado and Doctor (Ph.D.) degrees in physics, with specialty in electronics, from the University of Seville, Seville, Spain, in 1996 and 2002, respectively.

In 1995, he was a Graduate Student of the Spanish Ministry of Education at the Institute of Microelectronics of Seville (IMSE), National Microelectronics Center (CNM), Spanish Microelectronics Center (CSIC), Seville, where he also received a doctoral grant from 1997 to 1999, which was funded by the Andalusian Government, and where he is currently with the Department of Analog and Mixed-Signal Circuit Design. From February 2000 to June 2004, he was an Assistant Professor with the Department of Electronics and Electromagnetism, School of Engineering, University of Seville and at the Faculty of Physics. Since June 2004, he has been a Tenured Scientist of the Spanish Council of Research. His main areas of interest include the design and VLSI implementation of massively parallel analog-/mixed-signal image processors.

Dr. Liñán received the "1999 Best Paper Award" and the "2002 Best Paper Award" from the *International Journal of Circuit Theory and Applications*. He is also a corecipient of the "Most Original Project Award" and the "2002 Salvà i Campillo Award," which were conceded by the Catalonian Association of Telecommunication Engineers.

Ángel Rodríguez-Vázquez (M'80–SM'95–F'96) received the Ph.D. degree in physics–electronics from the University of Seville, Seville, Spain, in 1983.

He is a Full Professor of electronics with the University of Seville and the Head of Innovaciones Microelectrónicas S.L. (AnaFocus). He founded and headed a research unit on High-Performance Analog and Mixed-Signal VLSI Circuits of the Institute of Microelectronics of Seville (IMSE), National Microelectronics Center (CNM). His team made pioneering R&D activities on bioinspired microelectronics, including vision chips and neuro-fuzzy interpolators and controllers. His team also made significant contributions to the application of chaotic dynamics to communications, including the design and production of the first worldwide chaos-based communication modem chips. Some 30 high-performance mixed-signal chips were successfully designed by his team during the last 15 years in the framework of different R&D programs and contracts. These include three generation of vision chips for high-speed applications, analog front ends for XDSL modems, ADCs for wireless communications, ADCs for automotive sensors, chaotic signal generators, complete modems for power-line communications, etc. Many of these chips are state-of-the-art in their respective fields. Some of them entered in massive production. In 2001, he was one of the cofounders of AnaFocus, a high-technology company focused on the design of mixed-signal circuits, with emphasis on CMOS smart imagers and bioinspired vision systems on chip. He has been heading Anafocus since 2004. He has authored or edited 8 books; around 40 chapters in contributed books, including original tutorials on chaotic integrated circuits, design of data converters, and design of chips for vision; and more than 400 articles in peer-reviewed specialized publications.

Dr. Rodríguez-Vázquez has served as Editor, Associate Editor, and Guest Editor for different IEEE and non-IEEE journals, as Chairman for different international conferences, and is a member of the committees of some international journals and conferences. He has received a number of international awards for his research work (including the IEEE Guillemin-Cauer Best Paper Award) and was elected Fellow of the IEEE for his contributions to the design of chaos-based communication chips and neuro-fuzzy chips.